CSVTU Research Journal ISSN: 0974-8725 Vol. 9(2), 120–135, 2020

Reviews on the Friction Stir Welding Process that Affects Various Parameters

Rasbihari Vishwakarma[1], Sharda Pratap Shrivas[1], G K Agrawal[2], S Nagpal[3]
[1]Department of Mechanical Engineering, Chouksey Engineering College Bilaspur,
[2]Department of Mechanical Engineering, Government Engineering College Bilaspur,
[3]Department of Mechanical Engineering, Bhilai Institute of Technology Durg
Corresponding Author; Email: rasbihariv@gmail.com
Received August 31, 2020; received in revised form Jan 05, 2021; Accepted Jan 13, 2021

Abstract
A friction stir welding (FSW) is clearly an important process for the success of welding. Many common problems of fusion welding are overcome by friction stir welding (FSW), a widely used solid state joining process for soft materials such as aluminum alloys. The commercial achievability of the FSW process awaits the expansion of cost-effective and durable equipment for rigid alloys such as aluminum that lead to structurally sound welds. Material assortment and design significantly affect weld quality and cost. In this review several important aspects of FSW equipment such as equipment material selection, geometry and load carrying capacity, thermal behavior, equipment reduction mechanisms and process economics.
Key Words: - Friction stir welding, tool effect, microstructure, welding strength, welding parameter

1. Introduction

It was invented in 1991 at TWI (The Welding Institute), initially for aluminium joining. Comprehensive reviews about FSW process can be found in various literatures its schematic diagram shown in fig 1. The basic concept of FSW is a non-consumable rotating tool, especially designed with a geometry consisting of a pin and recess (shoulder) (Batalha et al., 2012). FSW can induce frictional heat and plastic metal flow, generating dynamic re crystallization, grain refinement, and second phase refinement that enhances the mechanical properties of materials. One of the most commonly tool used in FSW high-speed tool steels. Under high-speed conditions, it can still maintain good mechanical properties, and its price is lower than that of TCC, so it is often used as a stirring tool in FSW (Chen et al., 2019). Friction stir welding tool used to weld high melting temperature materials, such as steels and titanium alloys, must be capable enough to withstand the high shear and impact forces as well as high wear resistance at elevated temperature. Since there is no bulk melting of the work piece, the common problems of fusion welding such as the solidification and liquation cracking, porosity and the loss of volatile alloying elements are avoided in FSW. These advantages are the main reasons for its widespread commercial success for the welding of aluminium and other soft alloys.Though successful welds could be made using the above mentioned tool materials, the costs of such high end materials are very high due to difficulty in manufacturing of these tools. (Lakshminarayanan et al., 2014).

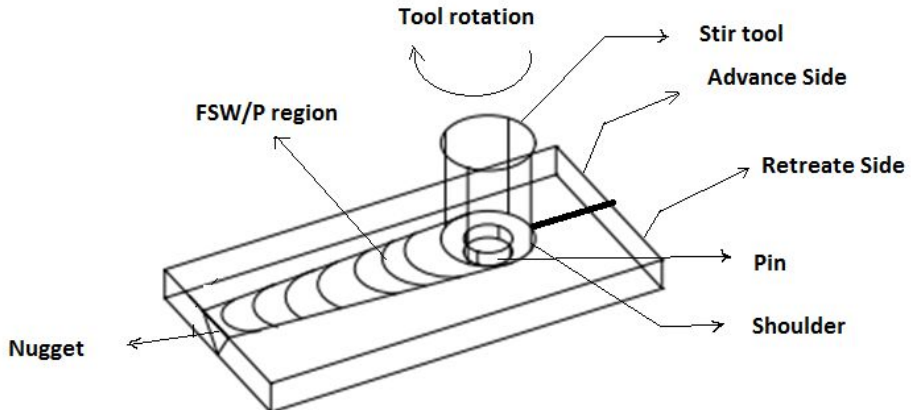

Fig. 1 Schematic Diagram of the friction stir process

2. Literature Review

Batalha et al. (2012) evaluated the performance of a vapour deposition (PVD) coating. Cement Carbide (WC) Equipment FSW Friction Alloy Welding uses friction welding equipment in the processing of TI alloy sheets. A coating of AlCrN material was applied to the WC device to improve its wear resistance, thermal shock stability and hot hardness. Tool demotion was evaluated for micro core microscopy to allow electron core strength to observe the wear mechanism. The actual profitability of the (Al, Cr) N coating layer cannot be evaluated, as the squire tool has no trace of its components. Pins and shoulder-wrapped element correspondence with EDS and titanium plate materials were traced back to the past after FSW. Chen et al. (2019) investigate on friction occurs when friction stir welding (FSW) joins the surface of the material temperature at that location. The conventional joining process in FSW even further freezes, partly increasing the melting point temperature on the metal. This friction can also clean plastic metal from heat smoke, it causes aggressive reintegration. On this paper we find that overlaying has affected the degree of diet effect of the two term substrate and the second will have a layer of overlaying and we have observed the interface in the zero set region and overlaid the forward direction. The resulting composition and micro hardness the subsurface of the coated samples was analyzed. Lakshminarayanan et al. (2014) studied to modify the surface of the FSW tool material by providing refractory composite coatings deposited using APS and PTA hard facing processes. The carbide powders, namely tungsten carbide, chromium carbide, boron carbide, titanium carbide and boron nitride, were chosen for coating and hard facing purposes. Li et al. (2017) evaluated Due to friction stir welding process in spindle, large amount Production of friction stir device for heat, and this welding thermal efficiency is very low and reduced welding thermal efficiency and resulting disastrous effects on spindle bearings. Using Finite Element Analytical Reproduction for Welding Devices for Friction Stirring in the Future Heat cushions study. We can see that three types of methods of stopping the heat flow from the tool to the spindle were studied and that the coating providing the thermal hangs of the device Barrier layer, that tool cross section area decreasing and also tool holder and tool shank. We observed three methods under the control of this experiment which were found based on analytical simulations and the transfer of heat equipment with the tool holder. Fall et al. (2016) studied that looked at equipment wear rate and wear rate in FSW during

welding according to friction stir The Ti-6Al-4V alloy is studied. In this process the shape of the conical tungsten carbide tool produced the butt-type. The friction stirrer moves the joints on the 2 mm thick Ti-6Al-4V body. And it is also believed that an original design was the movable pin, which caused examination damage to the instrument in the event of a process. Device movement we seen that reducing quality at welded joints. And discuss the microstructure of the welded surface of the material.

A.M. Sadoun et al. (2019) shows friction stir welding (FSW) devices processing different surface ephemeral temperatures were effectively measured at the top of the surface during the FSW, and the midpoint of the sample thickness, and the centre at the bottom surface. In that case the results show an unproductive value of the pin side area, which is defect free in the FSW 7075-O process of the 7075-O AL alloy range, with a 50 mm / min welding speed at 500 rpm. The pin area is the high side of the result, resulting in higher tensile strength in the semi-circular pin, with a higher proportion (29.83%) of the pin side area generated at the FSW process joint with higher tensile strength. Salloomi et al.(2020) studied the performance was accurate to finite element simulation to prevent temperature distribution and coercing Strain during friction stir welding (FSW) of AA 7075-T651 alloy. And analyze the process of individual steps, including spindle and tool techniques such as plumbing, welding, and travel setups, such as arbitrage Lagragian – eulerian (ALE) formulations, the contact between the welding tool and the work piece was modelled through applying nonlinear friction to the coefficient value. And also different types of material properties and heat transfer losses due to thermal contention conduction process between work pieces. Sorger et al. (2017) investigated that modern high-strength steel has a reduction in weight without compromising the development of load carrying capacity. FSW had joined the HSS in low altitude temples should be base material to better preserve the properties of the base material. We observed that HSS has a variety of extreme temperatures and cooling rates on its properties. HSS was produced by a thermo mechanically controlled process, which was welded by FSW with peak temperatures that measurement, tinted, within the processed area. Tarasov et al.(2014) done an investigation the diffusion wear mechanism in 1.2344 X40CrMoV5-1 steel FSW equipment. It performs standpoint cognition generation of different layers in the tool. It has been observed that the surface layer of the working layer of specification of iron or aluminium under AMg5M temperature in aluminium alloys and the mechanical stress hanging pre-grain boundaries under makeup also increase rapidly. Chegeni & Kapranos(2017) experimented used a Two rolled aluminium plate in 7075 series, then both plates are welded using a coexistent double-side in the FSW process. We had seen that properly feedstock material to semi-solidified reaction with oxygen atoms for deformation in the case that partial melting takes place at some point Semi-solid state. Both the base plate material and the friction welded area had deformation at 628 subject to welding heat treatment at the limit of temperature at 628° C. Maa et al. (2014) performed the UFG 7075 materials show higher quality than the CG 7075 materials in every proportional condition. The quality of the as-expelled UFG 7075 (YS: 583 MPa, UTS: 631 MPa) is considerably higher than business Al 7075 with the T6 temper (YS: 541 MPa, UTS: 593 MPa) and is close in an incentive to the CG 7075 example with the T6 temper (YS: 613 MPa, UTS: 659 MPa). After a T6 temper, both the UFG and CG 7075 materials display a significant increment in quality.

The YS and UTS of test UFG7075-E-T6 are 734 and 774 MPa, individually, which are 120 MPa higher than those of test CG7075E-T6 (YS: 613 MPa, UTS: 659MPa). The age-solidifying impact, for example the quality addition after common maturing or T6 temper, in the UFG 7075 materials isn't, be that as it may, as noteworthy as that in the CG 7075 materials. The increments in yield quality of tests CG7075-E-Nag and CG7075-E-T6 are 70% and 160%, individually, relative to that of CG7075-E-sol. Conversely, the increments in yield quality after common maturing and T6 temper for the UFG 7075 materials are as it were 13% and 26%, separately. Ambroziak et al. (2014) The distinctive examination gives that can happen during contact welding of different materials were portrayed in this paper. The basic impacts during welding, mechanical properties of joints, and various setups of the procedure so as to acquire great welds were investigated. The investigation of the aluminium-iron double framework prompts he end that long time and high temperatures of the procedure can cause the arrangement of intermetallic phases. They are probably going to be the explanation behind fragility of joints. Contingent upon the kind of joined materials and the procedure boundaries distinctive metal mixes having various properties might be framed. Sivaraj et al. (2014) studied Friction mix welding for 12 mm thick moved plates of precipitation solidified, high quality protection grade AA7075-T651 aluminium compounds was prevailing with no imperfections utilizing single pass welding strategy. The malleable properties of erosion mix welded AA7075-T651 amalgam were weakened due to hasten disintegration because of frictional warming. The counterfeit maturing treatment (120 _C, 24 h) applied in this examination further decreased the pliable properties of contact mix welded AA7075-T651 aluminium compound joints. The arrangement treatment followed by counterfeit maturing cycle (480 _C for 1 h þ 120 _C for 24 h) is framed to be gainful to expand the pliable properties and hardness of rubbing mix welded AA7075 aluminium combination joints.

3. Effect on microstructure

Ilangovan et al. (2014) shows the impacts of hardware nail profile to microstructure and tractable properties of grating mix weld disparate AA 6061- AA 5086 aluminium composite joints were explored and the following ends are determined. Of the three device pin profile utilized, the straight round and hollow pin profile instrument yielded cross-sectional full scale level deformities in the mix zone and consequently isn't accessible for AA 6061 and AA 5086 different joints. Threaded and tightened tube shaped pin profile apparatuses yielded deformity free joints (both surface and cross-sectional). Kumar et al. (2015) performed in Friction mix welding of AA7075 combination with the expansion of boron carbide powder brought about the improved hardness and refinement of microstructure in piece zone. Microstructure of chunk zone was seen as receptive to the post weld heat medicines of pinnacle maturing (T6), retrogression and RRA.RRA treatment with the expansion of boron carbide powder brought about progress in hardness of weld chunk and the expanded hardness is ascribed to the uniform appropriation of reinforcing hastens in the network and molecule reinforcing. Rengarajan & Rao (2016) Two unique metals of AA7075 and AA6061 both in T6 conditions were welded utilizing strong state welding strategies (erosion welding) for various boundaries and a decent holding quality was accomplished. Radiography test was directed. All the examples were inside worthy cut-off points, aside from test 1 as it needed entrance and contained voids because of low rubbing pressure during

welding. The most extreme elasticity of 203 MPa was accomplished with high steamed weight, medium erosion weight, speed, and low consume off length esteems. Shah & Badheka, (2017) the researcher studied that temperature distributions in the work piece Al 7075 T651 were determined experimentally during the FSW process. It was observed that the temperatures on the advancing side of the weld are bit higher than that of the retreating side of the weld. Though it is extremely difficult to measure the temperatures at the weld line, an attempt has been made to determine the temperatures around the rim of the tool shoulder. From the study it can be concluded that the appropriate temperature for a defect free friction stir weld of Al 7075 T651 can be within the range of 375 - 4200C. The joints fabricated with 20mm shoulder diameter yield maximum joint efficiency. The experimental results obtained can be helpful to control various process parameters during FSW of Al 7075 T651 to achieve defect free, sound and good quality welds.

Bayazid et al.(2015) The effects of cyclic solution treatment (consecutive heating between 400 °C and 480 °C) followed by artificial aging on microstructure and mechanical properties of FSW and 7075 Al alloy were studied. It was found that FSW process deteriorated mechanical properties of the alloy, especially in HAZ and TMAZ. The CST extremely homogenized and recovered the mechanical properties of the joints without the occurrence of abnormal grain growth. The enhancement of mechanical properties via CST was attributed to the repetitive partial dissolution of large MgZn2 precipitates and formation of fine met stable MgAlCu precipitates. The preservation of the fine grain structure and the dispersion of fine stable MgAlCu precipitates after aging for 24 h at 130 °C caused a significant enhancement in hardness (39%), yield stress (11%), and ultimate tensile strength (10%) of the joints without a considerable change in the ductility compared with the base plate in T6 condition. Burek et al. (2018) done an investigation apparatus pin acts in the most troublesome conditions and is generally helpless to wear. The moderately little components of the pin like its 4mm width and the huge powers (5kN) that happen during process cause this part to be the most defenceless to wear. Moreover, string wear builds the odds of harm that can likewise feeble the apparatus centre. Face surface and circumferential wear of the device was seen during the welding procedure that was relative to the welding separation. Therefore, it is principal to control the pin expansion to guarantee the ideal weld quality boundaries during the procedure. During the underlying welding stages, the apparatus experienced a break in period over the principal 40m of welding that was portrayed by diminished quality. After this separation, the quality qualities balance out at around ~6.5kN. After 200m of welding, the welds' quality starts to diminish by about 30% and the repeatability of the outcomes additionally disintegrate in view of an adjustment in the blending states of the material (string wear influences the vehicle of the plasticized material). Chegeni & Kapranos (2018) shows the Plates of aluminium 7075 composite have been welded by a concurrent twofold sided grinding mix welding strategy. Since these welds experience broad plastic disfigurement, a post welding heat treatment was led in the semi-strong district at a temperature of 628 _C, so as to research if the resultant microstructures create along these lines those experienced in semi-strong metal handling or on the other hand thixoforming. The accompanying ends can be gotten from this examination: The base metal comprises of ordinary flapjack moulded grains prolonged the moving way however the grain size is fundamentally

diminished in the chunk zone because of broad plastic misshapening that the materials experience during FSW; Grains begin to develop all through the material during heat treatment at 628^{o}C, bringing about uniform non-dendrite microstructures like those got by thixoforming; Hardness tests show that hardness in the NZ is higher than that in TMAZ and BM due to the ultra-fine grain structure achieved here. Also Rasal (2017) experimental it very well may be infer that various kinds of welding procedure can be used so as to weld aluminium compound and steel. Investigation of mechanical properties of the weld, temperature, process boundaries are assumes significant job. The serious issue happens with aluminium and steel weld is the development of intermetallic mixes at the interface. It influences the properties and productivity of the weld. So as to improve the quality of these metals weld middle of the road layers at the interface can be utilized. Chandrana et al.(2018)The discoveries of this examination are: Torque and force utilizations increment following an expansion in the water head during the lowered erosion mix welding. The force esteems and force utilization are high in the lowered erosion mix welding contrasted with the typical grating mix welding. The prevalent weld morphology as onion ring design is accomplished during the lowered grating mix welding procedure and it isn't presenting the erosion mix welded tests.

Gong et al.(2019) Performed the vibration stress alleviating treatment followed by the ensuing characteristic maturing process has a noteworthy effect on diminishing the leftover pressure incited distortion in Al 7075 slight walled parts. As indicated by the outcomes acquired, vibration stress alleviation quickens the redistribution of lingering stresses which changed the disfigurement conduct of the parts, consequently viably alleviating the lingering stresses and improving shape solidness. Kacarb et al. (2019) in investigation, the impacts of maturing temperature, time, and pre-strain on mechanical properties are inspected for AA7075. The fundamental ends got from the examinations are as per the following: MgZn2 precipitation isn't seen at maturing temperatures of 120 and 160 ºC. At 200 ºC, MgZn2 encourage starts to be shaped following 30 minutes of maturing time and the measure of precipitation increments with expanding time. It is seen that the circulation of MgZn2 scatterings builds the quality. When maturing proceeded at a higher temperature or longer timeframe after the development of MgZn2 encourages, microstructure gets gentler. Cam & Mistikoglu (2014) over viewed the vast majority of FSW contemplates announced in the writing exceptional focused on FSW of Al-combinations, for which the technique is initially evolved. A huge loss of solidarity happens in the weld zone of these compounds after FSW, Table 4, both in the HAZ and SZ. The loss of solidarity in the HAZ district is because of the overaging in this locale because of warmth input This trouble is, be that as it may, inborn to precipitation solidified Al alloys and experienced in practically all welding forms. Besides, the base metal corruption in FSW isn't as high as that in combination welding forms including higher warmth inputs gave that ideal welding conditions to moderately bring down pinnacle temperatures are utilized. That is the reason FSW has just discovered striking modern application for Al-compounds and its mechanical use is relied upon to increment. By and by, erosion mix welding (comparative butt-, lap-, and spot welding applications in Al-composites) is now utilized modernly in assembling of boats, planes and space transports, trains, and different vehicles. The pertinence of FSW to join unique Al-combinations plates or Al-compounds plates with different materials, (for example, Mg-

composites) is as a rule as of now researched seriously. Along these lines, the headway accomplished around there (to be specific the advancement made in grinding mix butt-and spot-welding of Al-and Mg-composites, especially in disparate mixes) will make the large scale manufacturing of light transportation frameworks conceivable and thus critical decrease in fuel utilization will be accomplished. The welding strategy is additionally contender to supplant riveting in collections of planes. Cai et al.(2007) The connection between PFZ width and GB type with five boundaries was thoroughly researched by consolidated TEM estimations and OIM checks. Altogether, 502 GBs with a misorientation hub/point and PFZ width were acquired by TEM estimations. Among all GBs, 47 R GBs (up to R25b) as indicated by Brandon's standard and 36 low-edge grain limits (LAGBs or R1 GBs) were acquired. Taking all things together, 177,000 GB follows, recreated from OIM information, were utilized to recoup the GB plane appropriation by stereo logy. The level of the quantity of R GBs to all GBs is about 9.4% for both TEM and OIM factual results. The normal half width of PFZs at irregular GBs is 70.4 ± 0.7 nm. For R1 GBs, a clear change of PFZ width was found to happen at a mis-orientation h of 11_. This shows a structure change of GBs exists in this area. Subsequently, the R1 class was separated into R1(a) (2_ 6 h < 11_) and R1(b) (11_ 6 h < 15_). R1(a) can be viewed as the conventional LAGB with the littlest PFZ width. It additionally recommends that R1(a) GBs have the biggest dissemination initiation vitality of solute particles among all GB types. For other R GBs, the PFZ width of R3 and R5 is littler than that of irregular GBs, yet clearly bigger than that of R1(a).

Shah & Badheka (2017) founded the research that different distributions identified with FSW delineates the accompanying significant angles identified with FSW. Till date, an enormous bit of FSW considers revealed in the open writing centres around aluminium compounds for which the procedure was created. The procedure is most broadly utilized for welding of aluminium structures. The expansion in the quantity of down to earth uses of the procedure to join an assortment of aluminium structures in various fields of industry, particularly aviation ventures, has been featured. The procedure is equipped for delivering sound welds having numerous preferences over customary combination welding forms. The essentialness of shoulder to stick distance across proportion is likewise detailed. The usage of a bobbin device has demonstrated the possibility to conquer a portion of the impediments found in CFSW. The reasonable warmth profile in BFSW has capacity to create sound weld with much lower contortions and in this way the utilization of BFSW can be investigated particularly for joining thicker plates. It ought to likewise be recognized that the nonattendance of the sponsorship plate in BFSW expands its applications. The metallurgical and mechanical parts of both non-heat-treatable and heat-treatable aluminium amalgams are brought out. Be that as it may, the procedure turns out to be increasingly unpredictable for welding of precipitation solidified compounds as loss of solidarity because of encourages disintegration and coarsening is a significant issue. Over aging in HAZ is seen when these compounds are welded which signifies the issue. Improvement of such models could give critical stimulus to extra research in this field. The FSW procedure includes various interferential factors with nonlinear connections. The cooperation inside the elements is additionally prevalent in FSW. Man-made consciousness (AI) strategies have a more prominent capacity to catch nonlinear connections and are as often as possible utilized by specialists to gauge the yield reactions of different procedures.

Information produced from a trial study can be taken care of to AI strategies for the detailing of numerical models among input and the yield procedure boundaries. For instance, the AI models can be utilized to assess the disappointment loads and the quality properties of the joints. The utilization of AI strategies, for example, fluffy rationale and master frameworks would make it possible for the specialists and producers to focus their exertion in the improvement of innovations and hardware in FSW. Presentation of clashing interest's author proclaimed no expected irreconcilable situations as for the exploration, creation, as well as distribution of this article. Subsidizing The author(s) unveiled receipt of the accompanying budgetary help for the examination, initiation, or potentially distribution of this article: The writers wish to put their earnest gratitude to Indian Space Research Organization (ISRO), India, for monetary help rendered through the R&D. Record et al.(2007) This examination utilized factual experimentation to contemplate significant procedure boundaries what's more, the affectability of working conditions to these procedure boundaries. It is inferred that for the states of this investigation (device, material, techniques, levels, and so forth.): Spindle speed, feed rate, and plunge profundity are the three most critical components of the FSW procedure. Z-power is generally influenced by plunge profundity; feed rate and weld area had optional impacts. Spindle speed had no impact on Z-power. X-power is generally influenced by feed rate, trailed by pin length, and shaft speed. Shoulder temperature is generally influenced by shaft speed, trailed by pin length, plunge profundity, and feed rate. The area of the weld comparative with the sides of the plate influences Z-power.

Singh et al.(2018) performed FSW process, microstructure, remaining anxieties, mechanical properties, and uses of grating mix welding of Mg combinations have been tended to. The essential ends that can be drawn from this survey article are as per the following Tool geometry is the most persuasive piece of FSW process improvement. The device pin profile, shoulder measurement and device material exceptionally impacted the joint quality. The erosion between the device shoulder and work piece is the significant segment of warming. Along these lines, the size of pin and shoulder is a higher priority than the structure highlights of the apparatus. The looked over shoulder surface likewise assumed a huge job in mixing/mixing the material. The FSW procedure boundary (point of axle or instrument tilt regarding the work piece surface, target profundity and hub power, inclusion profundity), notwithstanding the apparatus revolution speed and cross speed, assumes a significant job in delivering sound welds. The material stream designs exceptionally relied on the geometry of the apparatus pin, welding temperature, material stream pressure and pivotal power. The welding temperature is reliant on the hub power. There is a ton of degree for research on the grounds that the joint de-signs like-edge butt joint, T butt joint, numerous lap joint, T lap joint, and filet joint separated from the butt and lap designs are likewise valuable in numerous applications. FSW adjusted the microstructure of the base metal and brought about the arrangement of weld mix zone (SZ), thermo-precisely influenced zone (TMAZ) and warmth influenced zone (HAZ). Each zone shows diverse smaller scale auxiliary qualities, including grain size, separation thickness, and remaining worry just as accelerate size and dissemination. Ciardiello et al. (2020) The mechanical conduct of cement joints arranged with a mono-part epoxy glue and U-shape boron steel substrates has been concentrated concerning five diverse stacking edges from unadulterated

tractable to shear tests. Two diverse relieving conditions were tried so as to survey if the temperature of the catachresis procedure is reasonable to fix the cement, so decreasing the time cycle. Mechanical tests demonstrated that there is no huge distinction between the cement relieved in the two unique conditions. The shear arrangement (0°) prompted the most noteworthy estimation of solidarity, with a decrease of 40% for the consolidated burden (45°) and half for the elastic configuration (90°). This decrease can be identified with the U-state of the substrates that, on account of the elastic test and the mixes shear-ductile, changes the method of break with a split way beginning from the sides and engendering towards the focal point of the security. This is particularly evident for the example broke in the test directed at 60°and 90°where the focal zone that looks darker is the last that isolated. DSC investigation demonstrated that both embraced restoring conditions can totally fix the cement and TGA shows that the empty glass circles and the minerals are available in a level of 35%. SEM examination was utilized to show the nearness of empty glass circles that are remembered for the glue grid by the maker. The scattering of these particles is uniform.

Chuaiphan & Srijaroenpramong (2020) investigation current work inspected the microstructure, mechanical properties and pitting erosion of TIG welded joints for an elective minimal effort 216 evaluation austenitic treated steel. The primary outcomes can be summed up as follows Austenitic treated steel grade Mn composite (SUS 216 minimal effort) can be welding by filler metal austenitic hardened steel grade Ni compound (SUS 316), proper for the tungsten idle gas (TIG) welding process. Because of it indicating no deformities in the weld metal examples and creating weld joints of high proficiency. For the concoction structures of all weld metals a huge validate of chromium equal and nickel proportional (Creq/Nieq) proportion at least 1.82 and most extreme 2.04. This is demonstrated the conduct of the hardening mode in the ferrite-austenite (FA mode) and similar with the estimations of ferrite anticipated by the Schaeffer graph. The microstructure of the weld metals comprised of delta-ferrite spread in an austenite framework stage which was the equivalent for all the welding conditions. In any case, for the weld metal the arrangement of delta-ferrite irregularity was more noteworthy for the medium and low warmth input levels. This was identified with the dendrite length and between dendrite dividing in the microstructure of the weld metal. This relates to the base metal having a lower pitting consumption potential than the entirety of the weld metal examples. Pitting was started at the interface region between the delta-ferrite and austenite and afterward pushed ahead in to the austenite stage.

M. Devrient et al. (2012) After a short inspiration a test strategy and arrangement for the portrayal of the dispersing conduct of thermoplastics subject to test materials, thicknesses and districts of test extraction comparative with the outside of the infusion shaped plates and furthermore comparative with the film entryway was presented. The strategy used to evaluate the dispersing conduct and to consider it inside a limited component model is contrasted with estimations did with the guide of a spectrometer and investigated by the Inverse-Adding-Doubling-Method moreover. It was seen that the factor ought to be characterized relied upon the facilitate and ward to the respected material because of changing conditions with respect to the infinitesimal structure of infusion shaped plates made out of semi crystalline thermoplastics like PP or PA 6. A short time later a procedure model on premise of the limited component strategy for laser transmission welding of

thermoplastics proficient to consider the trial portrayed dissipating conduct is presented. On premise of the information picked up by different reproductions did with this limited component model a systematic model competent to compute weld crease geometries subject to a few procedure boundaries just as upsetting amounts was deducted by the reaction surface strategy. Song et al. (2019) The CO2 laser welding of 2mm thickness TWIP980 steel sheets was broke down utilizing the trial and numerical reproduction strategies. The outcomes and investigation determine the accompanying ends By mimicking the temperature field of the laser welding of the TWIP980 sheet, the weld pool got is equivalent to the real weld, and it has a "nail head" shape. It shows that the warmth source model has great immaterialness. The expansion in the warmth contribution of the weld builds the width of the coarse-grained locale of the welded joint, so the weld heat information ought to be decreased while guaranteeing the weld quality. The lingering pressure produced by welding is chiefly amassed toward the path opposite to the weld crease. With the expansion of line vitality (heat input), the distortion of the sheet subsequent to welding increments, somewhere in the range of 0.09mm and 0.03mm. Lingering pressure and post-weld misshapening ought to be carefully controlled while guaranteeing infiltration. Through the laser welding re-enactment and examination of the temperature field and stress field of the TWIP980 steel, by looking at the state of the weld joint, the impact of the warm cycle temperature on the steel, the lingering pressure and the remaining bending, for the 2mm thickness TWIP980 steel sheet, the ideal welding process is with a welding power 3kW and a welding speed 3m/min. Extra exploratory confirmation is required, however the above examination additionally offers great hypothetical help and premise.

Lessa et al.(2020) The current work researches the viability of a two-pass Friction Stir Welding process, applied just because to API 5L X65 steel plates cladode with Inconel 625. Micro structural portrayal and mechanical tests were led and demonstrated an improvement of the mechanical properties in the weld area contrasted with the base materials. The accompanying key perceptions are made Limited material blending and between dispersion have been seen at the interface between Inconel 625 and API 5L X65 steel, because of the two-pass FSW strategy. The welding procedure changed the microstructure of the Inconel and the API X65 steel, where a recrystallized refined grains area was accomplished in the mix zone. A complex microstructure created by ferrite (F), bainite (B), Widmanstätten ferrite (W) and idiomorphic essential ferrite PF(I) was seen inside the steel weld. The FSW procedure forced change from a dendritic to an equi axial microstructure in the Inconel 625 weld. R.M. Afonso et al.(2020) Supervisor framing can be effectively used to deliver annular ribs in poles and dainty walled tubes. The procedure accumulates material into a pass on depression with controlled geometry and size, while the upper bite the dust moves along the hub heading, and is restricted by breaking or by plastic buck-ling in the particular instance of slender walled tubes. Disappointment by breaking is kept away from by restricting the width of the kick the bucket pit and by utilizing a pres-sure ring if there should arise an occurrence of the manager shaping of poles. Plastic flimsiness is likewise forestalled by constraining the tallness of the bite the dust hole to stay away from unreasonable thinness of the free segment of the slender walled tubes. The bar sheet and cylinder sheet joints are manufactured subsequent to getting the annular spines and the structure fit mechanical interlocking between the segments to be

joined by methods for a subsequent manager shaping activity or an upsetting of the free cylinder end against a countersunk or counter bored sheet gap, separately. Reisgen et al. (2020) performed the strategy for deciding the dynamic consistency of compounds with the assistance of direct spot-FSW preliminaries has been proposed. It depends on the estimations of the fashion power and force at the painless turning instrument, just as the thickness of the mix zone from the exploratory micro sections. The numerically based strategy permits in the end handling the tentatively gotten information and resulting figuring of an assortment of discrete qualities for the dynamic consistency in the mix zone in reliance on the temperature and strain rate at different estimations of the rotational speed and manufacture power. The guess of this information has given a logical estimation of the dynamic consistency being reasonable for use in CFD models of the FSW procedure. The got estimations of the dynamic thickness for AA5083 don't negate to the general hypothetical estimations of the property and connect subjectively well with the writing information for the amalgam AA6061. Smith et al., 1999 In the following phase of our work, they got model of the dynamic thickness for AA5083 will be executed into the total model of the FSW procedure.

4. Weld Zone Response

Baratzadeh et al. (2020) showed weld joints between AA6082-T6 and AA6063-T6 were delivered dependent on the enhanced weld boundary results from a structure of-explore process. Regarding the hardness profile of the joint, the most reduced estimation of hardness was acquired in the weld zone. This area relates to the area of the weld division when lap shear testing the unique lap weld joints. In the shear lap tests, come up short urea detachment happened in three distinct modes, including: (1) in the chunk of the weld, where the base measure of the hardness was watched (mode 1); (2) in the TMAZ of the weld on the withdrawing side, where the conceivable snaring impact impacts the partition of the weld and where the most elevated measure of the pressure dissemination was seen in this zone (mode 2); and (3) in the base (parent) material of the spec-miens (mode 3). For propelling side stacked sort an example, the joint effectiveness of T6 heat-rewarded examples was 3% higher than normally matured examples and 5% over as-welded examples. For propelling side stacking of type B examples, the joint effectiveness expanded 7% in re-sponge to the warmth treatment contrasted with the normally matured condition, and 11% contrasted with the properties of as-welded examples. Material stream, blending of the two amalgams, and the nonattendance of snaring were plainly distinguished in the micro structural examination of the divergent lap joint.

F. Weber et al. (2020) the procedure furthest reaches of liquid based joining are broadened effectively by the idea of external pressurization with better openness. Chuaiphan & Srijaroenpramong et al. (2020) contemplated the impact of hydrogen in argon as shielding gas for welding austenitic tempered steel grade SUS 201 through the GTA welding process. The accompanying ends can be drawn from this examination. The expanded of hydrogen blended in argon protecting gas caused an expansion in the size of the weld pool during welding as a result of expanded warmth input more than when utilizing unadulterated argon gas for protecting gas. The weld dot size marginally expanded with an expansion of hydro-gen blended in argon protecting gas combined with a speed up. It is brought about by adjusting heat contribution to the weld pool (high hydrogen makes high warmth input, while high welding speed

makes low warmth contribution to the weld pool). The expansion of hydrogen blended in argon protecting gas brings about (1) weld metals to build the territory of HAZ and (2) diminishes the grain course opposite to the line of FB in light of the hardening rate, and (3) weld zone, the delta – ferrite somewhat diminished on account of adjusting heat contribution to the weld pools be-tween increment in hydrogen gases and speed up.

C.Y. Wang et al. (2020) a 3D FEM model considering unpleasant surfaces is created to mimic and break down the temperature field, liquid pool geometry and stream fields in the LTW procedure, and the re-enactment results are in acceptable concurrence with the exploratory outcomes. The outcomes show that the welding temperature field shows that the temperature of the contact surface between the straightforward part and the permeable layer is broken, which is predictable with the fragmented contact of the contact surface under genuine welding conditions. The greatest stream rate in the welding district increments with the expansion of laser power diminishes with the speed up, and increments gradually with the increment of clipping power in the scope of 0–0.24 MPa. The reproduced weld width considering unpleasant surfaces is inacceptable concurrence with the test weld width. Therefore, the set up model can be utilized to anticipate the trial after-effects of laser transmission welding thinking about unpleasant surfaces.

Mannucci et al. (2020) performed the utilization of a vanadium interlayer related with twofold pass welding permitted acquiring safe joints among titanium and hardened steel with a joint coefficient of 100 % in regards to crude vanadium. A bendable crack happened in the remaining vanadium embed, when the measure of vanadium in the softened zone didn't surpass 30 at.% V. The nearness of HAZ in the unbelted vanadium didn't debilitate the addition, and the joint coefficient arrived at 100% contrasted with starting covered vanadium. The welds among titanium and vanadium contained cubic (Ti, V) strong arrangements and were liberated from inter metallic stages. The development of martensitic structures in HAZ of Ti-6Al-4V didn't actuate cracks during the pliable test. The welds among vanadium and 316 L contained just cubic (Fe, V) strong arrangements in any event, for low (6 at % V) weakening of supplement. The pillar balance on 316 L permits break free columnar hardening opposite to the furthest reaches of the softened zone, when a focused bar position created columnar structures close to 316 L side and coarse equiaxed grains in the remainder of the dissolve. The bar balance on vanadium created a dissolved zone with 47 at % V with expanded. M. Kuball et al.(2020) shows the Raising the procedure temperature has less impact on the strain solidifying conduct of 1.3815 than of 1.4541. By and by, the shaping of the high nitrogen steel at 200 °C rather than room temperature prompts a noteworthy decrease of the genuine pressure required for arriving at a similar genuine strain. The temperature impact on the yield quality is considerably higher for 1.3815 than for 1.4541. Furthermore, it was discovered that there is a straight reliance between the procedure temperature and the yield quality of the high nitrogen steel between room temperature and 200 °C. The Hockett–Sher by guess is a proper methodology for the extrapolation of the genuine pressure – genuine strain bends of 1.3815. It shows a sufficient exactness in the temperature scope of room temperature up to 200 °C. There is basically no contrast between the grating elements for 1.3815 and 1.4541 in contact with the tungsten carbide instruments at room temperature. The ascent in temperature up to 200 °C, in any case, prompts a critical increment of the grinding factor for the two materials.

5. Conclusion

Although tool design affects weld properties, defects and forces on the tool, the heat generation rate and flow of plastic in the work piece are influenced by the shape and size of the tool shoulder and pin, and currently empirically by trial and error Are designed. Work on the systematic design of tools using scientific principles is just beginning. Examples of recent studies include calculation of flow fields for different tool geometries and the calculation of tool shoulder dimensions based on the tool's grip of the plasticized material. The pin cross-sectional geometry and surface features such as threads influence the heat generation rates, axial forces on the tool and material flow. Tool wear, deformation and failure are also much more prominent in the tool pin compared with the tool shoulder. The axial, longitudinal and lateral forces on the tool can be calculated as functions of process parameters, or evaluated from the measured data. Estimation of the load bearing ability of the tool pin is needed considering the maximum stresses in the tool pin due to combined effects of bending and torsion. There is a need for concerted research efforts towards development of cost effective durable tools for commercial application of FSW to hard engineering alloys.

References

1. Afonso, R.M., Alves, L.M., Martins, P.A.F. 2020 Joining by boss forming of rods and tubes to sheets. Journal of Advanced Joining Processes. doi.org/10.1016/j.jajp.2019.100001.
2. Ambroziak, A., Korzeniowski, M., Kustron, P.B., Winnicki, M., SokoBowski, P.B., Harapinska, E. 2014. Friction Welding of Aluminium and Aluminium Alloys with Steel. Hindawi Publishing Corporation Advances in Materials Science and Engineering, (2014): 01-15, doi.org/10.1155/2014/981653.
3. Baratzadeh, F.,Boldsaikhan, E., Nair,R., Burford, D., Lankarani, H. 2020. Investigation of mechanical properties of AA6082-T6/AA6063-T6 friction stir lap welds. Journal of Advanced Joining Processes 1 (2020): 01-07, doi.org/10.1016/j.jajp.2020.100011.
4. Batalha, G.F., Farias, A., Magnabosco, R., Delijaicov, S., Adamiak, M., Dobrzański, L.A. 2012. Evaluation of an AlCrN coated FSW tool. Journal of Achievements in Materials and Manufacturing Engineering, 55(2): 607-615.
5. Bayazid, S.M., Farhangi, H., Asgharzadeh ,H., Radan ,L., Ghahramani, A. Mirhaji,A.2016. Effect of cyclic solution treatment on microstructure and mechanical properties of friction stir welded 7075 Al alloy. Materials Science & Engineering A 649/2016 : 293–300.
6. Burek,R., Wydrzyński,D., SępWojciech,J., Więckows. 2017. The effect of tool wear on the quality of lap joints between 7075 t6 aluminum alloy sheet metal created with the FSW method. Eksploatacja Niezawodnosc Mainten ance and Reliability, 102 Vol. 20, No. 1, 2018. :101-106.
7. Cai, B., Adams,B.L., Nelson,T.W. 2006. Relation between precipitate-free zone width and grain boundary type in 7075-T7 Al alloy. Acta Materialia 55 (2007): 1543–1553.
8. Cam, G., Mistikoglu,S.2014. Recent Developments in Friction Stir Welding of Al-alloys. Journal of Materials Engineering and Performance, DOI: 10.1007/s11665-014-0968. 23, (6): 1936-1953.
9. Chandrana, R., Kumar, S., Santhanamb, V. 2018. Submerged Friction Stir Welding of 6061-T6 Aluminium Alloy under Different Water Heads. Materials Research. 2018; 21(6): 01-11.

10. Chegeni, A.A., Kapranos,P.2017. A Microstructural Evaluation of Friction Stir Welded 7075 Aluminum Rolled Plate Heat Treated to the Semi-Solid State. Metals 2018, 8, 41; doi:10.3390/8010041 : 01-09.
11. Chegeni, A.A., Kapranos, P.2018. A Microstructural Evaluation of Friction Stir Welded 7075 Aluminum Rolled Plate Heat Treated to the Semi-Solid State. Metals 2018, 8, 41: 01-09.
12. Chen, K.J., Hung. F.Y., Lui, t.s., Shih, Y.R. 2019. Wear inducing phase transformation of plasma transfer arc coated tools during friction stir welding eith AL alloy.journal of engineering: 01-10.
13. Chuaiphan, W., Srijaroenpramong, L.2020. Microstructure, mechanical properties and pitting corrosion of TIG weld joints alternative low-cost austenitic stainless steel grade 216. Journal of Advanced Joining Processes, S2666-3309(20)30025. doi.org/10.1016/j.jajp.2020.100027.
14. Chuaiphan ,W., Srijaroenpramong, L.2020. Effect of hydrogen in argon shielding gas for welding stainless steel grade SUS 201 by GTA welding process. Journal of Advanced Joining Processes 1 (2020) 100016: 01-08.
15. Ciardiello, R., Greco, L., Miranda, M., Sciullo, F.D., Goglio, L,2020. Experimental investigation on adhesively bonded U-shaped metallic joints using the Arcan test. Journal of Advanced Joining Processes 1.2020/100010.
16. Devrienta, M., Dab, X., Fricka, T.,c, Schmidta,M.2012. Experimental and simulative investigation of laser transmission welding under consideration of scattering. Physics Procedia 39 (2012) 117 – 127.
17. Fall, A., Fesharaki, M.H., Khodabandeh, A.R., Jahazi, M.2016. Tool Wear Characteristics and Effect on Microstructure in Ti-6Al-4V Friction Stir Welded Joints. Giuseppe Casalino, doi:10.3390/met6110275: 1-12.
18. Gong, H., Sun, Y., Liu, Y., Wu, Y., He, Y., Sun, X., Zhang, M.2018. Effect of Vibration Stress Relief on the Shape Stability of Aluminum Alloy 7075 Thin-Walled Parts. Metals 2019/ 9/ 27 : 01-12.
19. Kacar, I., Fahrettin, M.S., Erdema, O.2019. Effects of Aging Temperature, Time, and PreStrain on Mechanical Properties of AA7075. Materials Research, doi.org/10.1590/1980-5373-mr-2019-0006.
20. Kuball, C.M., Jung, R., Uhe, B., Meschut, G., Merklein, M.2020. Influence of the process temperature on the forming behaviour and the friction during bulk forming of high nitrogen steel. Journal of Advanced Joining Processes 1 (2020) 100023: 01-09.
21. Kumar, P.K., Reddy, G.M., Rao, S. 2015. Microstructure and pitting corrosion of armour grade AA7075 aluminium alloy friction stir weld nugget zone e Effect of post weld heat treatment and addition of boron carbide. Defence Technology 11 2015: 166-173.
22. Lakshminarayanan, A.K., Ramachandran, C.S., Balasubramanian, V.,2014. Feasibility of surface-coated friction stir welding tools to join AISI 304 grade austenitic stainless steel. Defence Technology dx.doi.org/10.1016/j.dt.2014.07.003: 1-11.
23. langovani, M., Boopathy, S.R., Balasubramanian, V.2015. Effect of tool pin profile on microstructure and tensile properties of friction stir welded dissimilar AA 6061eAA 5086 aluminium alloy joints. Defence Technology 11 2015: 174-184.
24. Lessaa, C.R.D.L., Landella, R.M., Bergmanna, L., Kwietniewskib, J.C.E.F., Regulyb, A., Klusemanna, B., Santosa ,A.F.D.2020. Two-Pass Friction Stir Welding of Cladded API

X65. Procedia Manufacturing 47: 1010–1015.
25. Li, H., Qin, W., Liu, D., Li, Q., Wu, Y.2017. Design of friction stir welding tools reducing heat flow into spindle. Int J Adv Manuf Technol, DOI 10.1007/s00170-017-0985-7: 1-8.
26. Maa, K., Wen, H., Hua, T., Topping, T.D., Isheim, D., Seidman, D.N., Lavernia, E.J., Schoenung, J.M. 2014. Mechanical behavior and strengthening mechanisms in ultrafine grain precipitation-strengthened aluminum alloy. Acta Materialia 62 2014: 141–155.
27. Mannucci, A., Tomashchuk, I., Mathieu, A., Bolot, R., Cicala, E., Lafaye, S., Roudeix,C.2020. Use of pure vanadium and niobium/copper inserts for laser welding of titanium to stainless steel. Journal of Advanced Joining Processes 1 (2020) 100022: 01-12.
28. Rasal, S. 2017. Welding of Aluminium Alloys 6061-T4 to Stainless steel AISI 304, An Overview. International Conference on Ideas, Impact and Innovation in Mechanical Engineering ICIIIME 2017 ISSN: 2321-8169 Volume: 5 (6): 1775-1780.
29. Recor, J.H., Covington, J.L., Nelson, T.W., Sorensenc, D., Webb, B.W. 2007. A Look at the Statistical Identification of Critical Process Parameters in Friction Stir Welding. Welding resurch 86: 97-103.
30. Reisgen, U., Schiebahn, A., Sharma, R., Maslennikov, A., Rabe, P., Erofeev, V. 2020. A method for evaluating dynamic viscosity of alloys during friction stir welding. Journal of Advanced Joining Processes 1 (2020) 100002: 01-09.
31. Rengarajan, S., Rao, V.S. 2015. Characteristics of AA7075-T6 And AA6061-T6 Friction welded joints. Transactions of the Canadian Society for Mechanical Engineering, Vol. 39 (4) 2015: 845-854.
32. Sadouna, A.M., Wagihb, A., Fathyb, A., Essac, A.R.S.,2019. Effect of tool pin side area ratio on temperature distribution in friction stir welding. Results in Physics 15 (2019) 102814: 1-8.
33. Salloomi, K.N., Hussein, F.I., Al-Sumaidae, S.N.A.2020. Temperature and Stress Evaluation during Three Different Phases of Friction Stir Welding of AA 7075-T651 Alloy. Hindawi Modelling and Simulation in Engineering, doi.org/10.1155/2020/3197813
34. Shaha,P.H., Badhekab,V.2016. An experimental investigation of temperature distribution and jointproperties of Al 7075 T651 friction stir welded aluminium alloys. Procedia Technology, 23 : 543 – 550.
35. Sivraj, P., Kanagarajan, D., Balasubramanian, V. 2014. Effect of post weld heat treatment on tensile properties and microstructure characteristics of friction stir welded armour grade AA7075-T651 aluminium alloy. Defence Technology 10 (2014): 01-08.
36. Shah, P.H., Badheka, V.J.2017. Friction stir welding of aluminium alloys: An overview of experimental findings – Process, variables, development and applications. Materials Design and Applications 0(0) : 1–36.
37. Singh, K., Singh, G., Singh, H. 2018. Review on friction stir welding of magnesium alloys. Journal of Magnesium and Alloys (6)2018 :399–416.
38. Song, Y., Wang, Y., Zhang, M.2019. Experimental and Numerical Simulation on Laser welding of High Manganese TWIP980 Steel. Procedia Manufacturing 37 (2019) 385–393.
39. Sorger, G., Sarikka, T., Vilaça, P., Santos, T.G.2018. Effect of processing temperatures on the properties of a high-strength steel welded by FSW.

Welding in the World, doi.org/10.1007/s40194-018-0612-8: 01-13.

40. Tarasov, S.Y., Rubtsov, V.E., Kolubaev, E.A.2014. Aproposed diffusion-controlled wear mechanism of alloy steel friction stir welding (FSW) tools used on an aluminium alloy. Wear318(2014): 130–134.
41. Wang, C.Y., Jiang ,C.Y., Wang, C.D., Liu, H.H., Zhao, D., Chen, Z.L. 2020. Modeling three-dimensional rough surface and simulation of temperature and flow field in laser transmission welding. Journal of Advanced Joining Processes 1 (2020) 100021: 01-10.
42. Weber, F., Hahn, M., Tekkaya, A.E. 2020. Joining by die-less hydroforming with outer pressurization. Journal of Advanced Joining Processes 1 (2020) 100014: 01-04.